# Reports

## The Surface Temperature of the Sun and Changes in the Solar Constant

J. R. Kuhn, K. G. Libbrecht, R. H. Dicke

**The solar distortion telescope has been used to measure the limb shape and latitude dependence of the limb brightness during the summer months for a 5-year period—a time base sufficient to detect solar cycle trends in the data. Comparison of these observations with spaceborne measurements of the solar constant suggests that a significant part of the solar cycle variation in irradiance is a result of temporal changes in the latitude-dependent surface temperature of the sun.**

Precise spaceborne measurements of the solar constant, that is, the solar irradiance as determined from the earth's orbit, have shown that it changes slightly with the changing level of magnetic activity on the sun (*1*). These measurements, specifically those made by the active cavity radiometer irradiance monitor (ACRIM) experiment aboard the Solar Maximum Mission (SMM) spacecraft, have shown that during a typical solar maximum the solar irradiance is 0.1% higher than at solar minimum when the sun's magnetic activity is low. Such changes may measurably affect the earth's climate—a decrease in solar activity in the 16th century was coincident with a period of cool temperatures in Europe known as the "little ice age" (*2*).

The irradiance variation is a result of temporal changes in the flux and the surface brightness distribution of the sun. Earlier work has shown that dark sunspots on the visible disk do diminish the solar constant; other indirect (proxy) indicators also show that the solar irradiance increases because of bright faculae (*3, 4*). These studies also suggest that solar cycle variations in the spots and faculae alone cannot account for the total variability.

Identifying the cause of this variation is a difficult problem—for example, temporal changes in differential rotation in the interior of the sun, a solar dynamo magnetic field near the base of the convection zone, or large-scale convective cells might all produce such an effect. However, observations of the surface temperature distribution of the sun can be used to distinguish the effects of each of these mechanisms. For example, a latitudinal temperature distribution characterized by large-scale quadrupolar variations could be related to solar differential rotation. Furthermore, brightness observations combined with helioseismological splitting data may allow the determination of the aspheric structure of the solar interior (*5, 6*). Sensitive observations of temporal and spatial brightness variations will thus lead to a better understanding of the solar convection zone. In this report, we combine precise relative photometric measurements of the solar disk with spaceborne absolute total irradiance measurements to investigate the latitude-dependent and solar cycle–dependent surface temperature of the sun.

Total irradiance measurements, such as those made with the ACRIM experiment, do not provide data on the brightness variations across the visible solar disk. For this information the space experiments are well complemented by ground-based observations. Ground-based relative photometry allows higher spatial resolution for long periods of time but cannot provide the temporal absolute bolometric stability of the space measurements because of the effects of the earth's atmosphere.

Because the changes in the irradiance through the solar cycle are a few parts in

J. R. Kuhn, Department of Physics and Astronomy, Michigan State University, East Lansing, MI 48824.
K. G. Libbrecht, Big Bear Solar Observatory, 264-33 California Institute of Technology, Pasadena, CA 91125.
R. H. Dicke, Joseph Henry Laboratories, Princeton University, Princeton, NJ 08544.

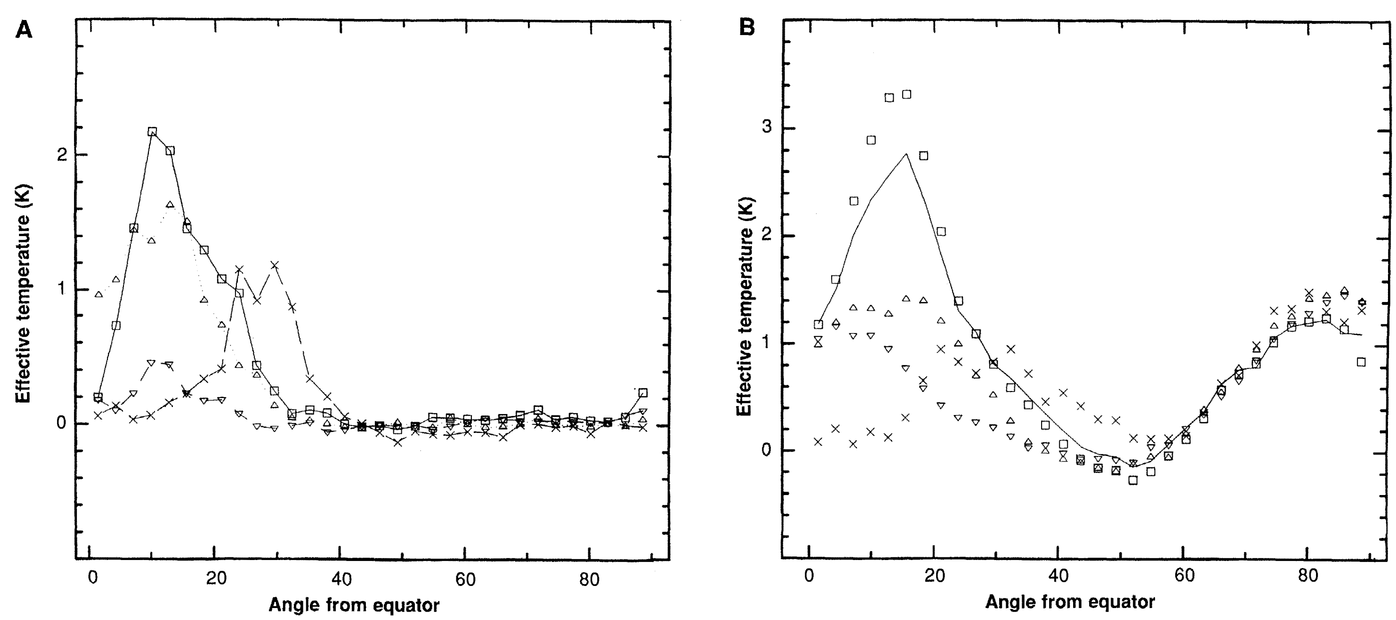


**Fig. 1.** Results of solar limb flux measurements from the solar distortion telescope between 1983 and 1987: squares, 1983; uptriangles, 1984; downtriangles, 1985; crosses, 1987. The errors at each point are about 0.2 K and are dominated by a systematic uncertainty in the brightness to flux calibration. (**A**) The measured effective temperature corresponding to the limb flux excess that results from faculae. (**B**) The measured limb temperature variation with latitude in Kelvin degrees. The solid line shows the result of a complete statistical fit to 1983 data (*8*).

$10^4$, a relevant measurement of the latitudinal flux variation must be of comparable accuracy. We have achieved more than adequate sensitivity in our measurements using the solar distortion telescope, an instrument that was originally designed to measure the oblateness of the sun with an accuracy of 1 arc millisecond (*8*).

This instrument has an occulting disk that blocks all but the outermost 20 arc seconds (0.02 solar radii) of the solar disk. The remaining solar limb flux can then be measured as a function of position angle around the solar disk. We measured the flux at 256 positions around the limb in two broadband color channels centered at wavelengths of 525 and 800 nm. By differencing the signals from the two colors, we expressed the data as an equivalent blackbody temperature excess as a function of solar latitude. Contributions to the flux signal from the solar oblateness and from refraction in the earth's atmosphere are significant, but the instrument design facilitates the separation of these systematic effects from the limb brightness signal (*8*). During a typical observing season, we made approximately $10^4$ 6-minute integrations, so that the statistical uncertainty of the measurements is small.

Using methods that were similar to those in (*8*), but modified for the 1987 data when fewer faculae were present on the sun, we divided the solar limb flux as a function of latitude into a "facular" and a "temperature" part. This was done with a statistical analysis that separated the data into (i) a latitude-dependent equivalent temperature excess, which was time-independent during a 4-month summer observation period, and (ii) intermittent bright regions, which are consistent with faculae passing over the solar limb. In this analysis, we considered the distribution function of the $10^4$ separate flux measurements at each point on the solar limb. We modeled the distribution function at each point as consisting of two parts: an approximately Gaussian distribution with a mean at the effective temperature excess, and a broader distribution that was the result of intermittent facular bright points (Fig. 1). The analysis yielded temperature excess curves (Fig. 1, A and B), which were normalized so that their sum yielded the total observed limb flux excess, independent of the identification of facular and thermal contributions.

The facular signal is confined largely to the active latitudes and has the expected dependence on the solar cycle (Fig. 1A). In the extreme polar regions the facular signal is elevated slightly, perhaps because of the presence of polar faculae (*9*). In our solar limb observations the flux deficit from sunspots was small compared to the excess from faculae because of the Wilson depression (*10*)–the greater continuum optical depth of sunspots makes them difficult to see near the limb.

**Table 1.** Fractional solar flux variations from 1983 to 1987. Column 1 is the mean time of each observation; column 2 is the change in flux (relative to 1983.5) measured by the ACRIM experiment; in column 3 the ACRIM flux has been corrected for the sunspot flux deficit, with the sunspot blocking function of (*4*). The large errors in this column reflect the uncertainty in the sunspot correction. Column 4 shows the calculated flux variation from our limb photometry when the low-latitude temperature signal is assumed to result entirely from faculae; column 5 shows the relative solar constant change if the facular and thermal contributions from Fig. 1, A and B, are used. The systematic errors are estimated from the sum of our calibration uncertainty, the variance in the daily sunspot correction, and the scatter in the published facular contrast functions. Estimated errors apply to all entries in each column.

| Date | ACRIM ($\times 10^4$) | Spot-corrected flux ($\times 10^4$) | Facular model ($\times 10^4$) | Temperature model ($\times 10^4$) |
|---|---|---|---|---|
| 1983.5 | $0 \pm 0.1$ | $0 \pm 0.1$ | $0 \pm 0.4$ | $0 \pm 0.3$ |
| 1984.5 | −2.1 | −4.1 | −1.0 | −3.8 |
| 1985.6 | −3.5 | −6.5 | −2.0 | −5.8 |
| 1987.6 | −3.0 | * | −1.6 | −5.4 |

*Not available.

Our observations of intermittent bright points (Fig. 1A) are clearly recording faculae and active regions near the limb. The remaining temperature signal is not as easily interpreted. The temperature signal consists of two parts (Fig. 1B): a high-latitude temperature excess, which varies little with solar cycle, and a low-latitude part, which occurs in the magnetically active latitudes and has a solar cycle dependence that is similar to that of the facular signal.

We have argued that the signal at high latitudes (above 50°) is a real temperature shift caused by a meridional circulation (*11*). The new data continue to support this interpretation of the high-latitude results but indicate that there is a second, variable, large-scale contribution to limb brightness near low latitudes that is also distinct from the facular and sunspot brightness components.

One criticism of this interpretation of the high-latitude data has been that polar faculae might produce the observed high-latitude temperature excess (*12*). With the new data, two pieces of evidence suggest that this explanation is unlikely. First, the brightness distribution of the high-latitude measurements is as narrow as the distribution near the mid-latitudes, in contrast to the wide distributions typical of the active latitudes (*11*). In other words, the distribution of the individual flux measurements at the poles is shifted upward in mean brightness, but it is not broadened as would be expected if this shift were caused by occasional polar faculae. Second, the polar brightness excess shows essentially no dependence on solar cycle, unlike the polar faculae. This latter point will be conclusive if the polar brightness excess remains unchanged through solar maximum, around 1991, when the polar faculae should disappear entirely (*9*).

In low-latitude data obtained after 1983, we did not completely separate the temperature component from the facular signal because too few faculae were observed to be able to statistically resolve them. However, by comparing the simplified analysis discussed here with the complete 1983 statistical analysis (indicated by the solid line in Fig. 1B), we conclude that at most ≈15% of the temperature signal can be associated directly with faculae. We show below that a comparison of these results with ACRIM observations supports the conclusion that the low-latitude bolometric temperature varies with the solar cycle. The source of this thermal flux is spatially unresolved by our observations and might be associated with the active magnetic network (*4*).

Between 1983 and 1987 the fractional change in the solar constant was $3.6 \times 10^{-4}$ (*1*). That the solar constant began increasing again after solar minimum is convincing evidence that the solar irradiance varies with the solar cycle. A shift of 0.5 K in the global mean solar temperature could have caused the observed luminosity variation. Because there already is evidence for a latitudinal brightness variation of this magnitude, we favor a changing latitudinal temperature distribution as a more likely mechanism causing the observed irradiance change. Models of the ACRIM data (*3, 4*) suggest that faculae and sunspots produce only some of the irradiance variation; thus, a third component is needed to account for the total variability.

In that sunspots are approximately uniformly dark, and their areas have been regularly cataloged for many years, the sunspot contribution to the irradiance, which directly reduces the solar constant, has been modeled accurately. However, because irradiance increases with increasing solar activity, the sunspot contribution is clearly not the dominant magnetic effect, and the effects of faculae and other small bright magnetic features on the irradiance are not as well known.

Ideally, precise relative photometry measurements covering the entire visible disk of the sun, coincident with the irradiance measurements, would allow the most accurate calculation of the facular contribution. Unfortunately, such observations have not been made. One advantage to our data is that the facular flux contribution is more easily identified in limb observations than in disk-center observations. We can then obtain the total solar flux by extrapolating our mean brightness measurements to disk center. To make this extrapolation, we used the solar limb darkening function, which is well known (*13*), and a facular contrast function, which is also fairly well known (*14–16*). If we assume that the flux brightness excess in the limb observations is a result of faculae and subject to a facular contrast function, then numerical integration shows that the magnitude of the solar flux variation implied by this facular model of the limb observations is too small to account for the decrease in the ACRIM data—even before the sunspot contribution to the ACRIM flux is accounted for (Table 1).

The uncertainties associated with the facular contrast that we assumed and the correction for the contribution of sunspots to the limb data are small compared to the difference between the facular model and the ACRIM data (columns 2 to 4 in Table 1). After the irradiance data have been corrected with an estimate of the sunspot blocking (column 3 in Table 1), the difference from the net irradiance, if we assume that our signal is caused by faculae entirely, is even larger. Thus we conclude that variations in ordinary faculae and sunspots alone could not have produced the observed changes in irradiance.

Instead, we suggest that a smoothly varying, effectively thermal flux excess (Fig. 1B) is the cause. Another integration over the solar disk, treating the data in Fig. 1B as a temperature excess not subject to a facular contrast function and the data in Fig. 1A as a facular signal, indicates (column 5 in Table 1 which should be compared with the spot-corrected irradiance flux, column 2) that the ACRIM variability is essentially accounted for. In other words, our interpretation of the limb brightness data as a temperature excess consistently accounts for the variability in the bolometric full disk ACRIM observations.

The limb data clearly indicate that latitudinal and temporal variations in faculae and sunspots could not have caused the total solar flux changes. A better description of the observed solar flux variation is in terms of a change in the effective temperature distribution of the sun at low latitudes. There is no evidence for a change in the solar flux in the polar regions (Fig. 2).

General considerations suggest that the solar flux is latitude dependent. Because the sun is differentially rotating in depth and latitude, the turbulent Reynolds stress in the convection zone has a large-scale angular dependence (*17*). A term of the force equation depends on the Reynolds stress; therefore, the momentum flux and the radial energy flux have a small quadrupolar angular dependence. The magnitude of the flux perturbation is difficult to calculate, and numerical simulations (*18*) have provided the best estimates of the form and magnitude of the observed flux excess (*11*).

This schematic picture suggests that the surface flux distribution is coupled to the solar rotation. It is an appealing ansatz for describing part of the temperature data in Fig. 1B. Because the solar rotation does not show a solar cycle dependence, a component of the flux excess should also be time independent, and the observed temperature excess at high latitudes does not vary with time. Extrapolating the high-latitude flux variation to the equator suggests that the temperature at the pole would be about 1.5 K hotter than at the equator if the low-latitude variable flux component were absent.

Two interesting features of the variable component of the temperature excess are that it peaks near the active latitude bands and that it varies on the same time scale as the solar magnetic field. Kilogauss-scale toroidal magnetic fields near the base of the convection zone may be long lived, and the time scale for small flux tube regions to drift to the surface could be comparable to the time scales over which active regions develop (*19*). Active regions, spots, and faculae occur where magnetic flux tubes break away from a large flux concentration deep in the convection zone and are carried by updrafts to the photosphere. In this case the active latitude bands should be located at the site of convective updrafts and these regions should be hotter than downdraft regions. In addition, the geometry and flux of the toroidal field in the deep convection zone will evolve during a solar cycle. We should expect a corresponding evolution of the surface temperature excess as the updraft region shifts with the changing dynamo field geometry at the base of the convection zone.

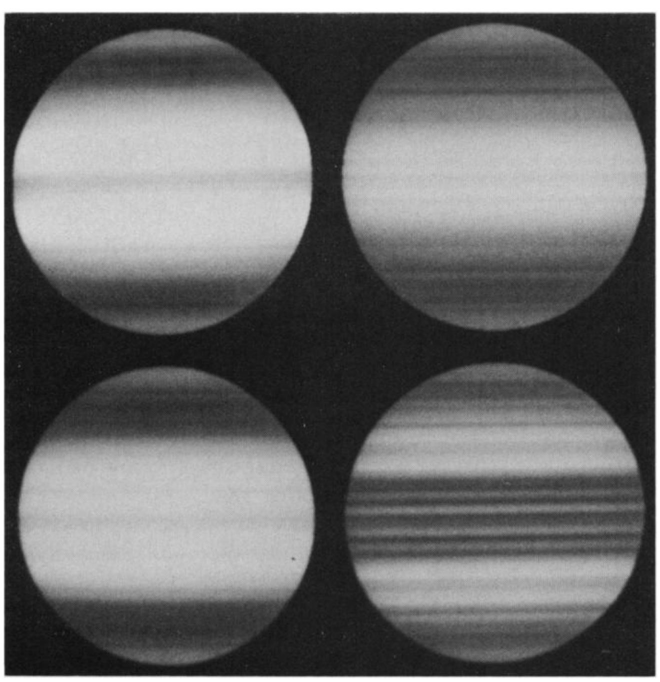

**Fig. 2.** The solar temperature distributions between 1983 and 1987. Sensitive measurements of the solar brightness between 1983 and 1987 at a wavelength near 500 nm and after removing faculae and sunspots would yield results corresponding to the patterns in this figure. The range from light to dark corresponds to a fractional intensity variation of about $2 \times 10^{-3}$. Starting in the upper left and moving down and then to the right column, the images correspond to the sun in the summers of 1983, 1984, 1985, and 1987.

REFERENCES AND NOTES


1. R. C. Willson and H. S. Hudson, *Nature* **332**, 810 (1988).
2. J. A. Eddy, *Climate Change* **1**, 173 (1977).
3. G. Chapman *et al.*, *Nature* **319**, 654 (1986).
4. P. Foukal and J. Lean, *Astrophys. J.* **328**, 347 (1988), and references therein.
5. J. R. Kuhn, *Astrophys. J. Lett.*, **331**, L131 (1988).
6. K. G. Libbrecht, *Astrophys. J.*, in press.
7. The instrument is a modified version of the telescope described by R. H. Dicke and H. M. Goldenberg [*Astrophys. J. Suppl. Ser.* **27**, 131 (1974)]. Additional information on the modified instrument is in (*8*) and K. G. Libbrecht [thesis, Princeton University (1984)].
8. J. R. Kuhn *et al.*, *Astrophys. J.* **290**, 758 (1985); *ibid.* **319**, 1010 (erratum) (1987).
9. N. R. Sheeley, *J. Geophys. Res.* **81**, 3462 (1976).
10. See, for example, E. G. Gibson, *The Quiet Sun* (National Aeronautics and Space Administration, Washington, DC, 1973), p. 40.
11. J. R. Kuhn, K. G. Libbrecht, R. H. Dicke, *Nature* **328**, 326 (1987).
12. B. J. Labonte, in *Solar Radiative Output Variations*, P.

Foukal, Ed. (National Center for Atmospheric Research, Boulder, CO, 1987), pp. 156–167.
13. C. W. Allen, *Astrophysical Quantities* (Athlone, London, 1976).
14. R. Muller, *Sol. Phys.* **45**, 105 (1975).
15. J. K. Lawrence and G. A. Chapman, in preparation.
16. K. G. Libbrecht and J. R. Kuhn, *Astrophys. J.* **277**, 889 (1984); *ibid.* **299**, 1047 (1985), and references therein.
17. B. R. Durney and H. C. Spruit, *ibid.* **234**, 1067 (1979).
18. G. Glatzmaier, *ibid.* **291**, 300 (1985).
19. E. N. Parker, *ibid.* **321**, 984 (1987); *ibid.*, p. 1008.
20. This research was supported in part by NSF grant ATM-8604400 and a Sloan Foundation grant to J.R.K.

25 July 1988; accepted 12 September 1988

# Enhancement of Surface Cooling Due to Forest Fire Smoke

Alan Robock

**Smoke emitted from forest fires in northern California in September 1987 was trapped in a valley by an inversion for 3 weeks. Daily maximum temperatures on the valley floor were more than 15°C below normal for 1 week and more than 5°C below normal for 3 weeks. The smoke strengthened the inversion by preventing surface warming by solar radiation, thereby enhancing the smoke trapping and the surface cooling in a positive feedback loop. These results may have implications for nuclear winter.**

Crutzen and Birks (*1*) were the first to suggest that smoke from forest, urban, and industrial fires ignited by nuclear weapons would be extensive enough to block out significant amounts of sunlight. The resulting surface cooling calculated with a climate model was so large that it was called "nuclear winter" (*2*). Smoke from urban and industrial fires (especially oil refineries) would be much more effective at preventing solar radiation from reaching the earth's surface than forest fire smoke after a large-scale nuclear war (*2, 3*); with both urban and rural targets, not only would more urban smoke be generated but its optical properties would make it more effective at blocking sunlight.

In this context, the effects of forest fire smoke are of interest for two reasons. First, a lot of forest fire smoke would still be generated in many nuclear war scenarios, especially those that include only nonurban military targets. The optical properties and surface temperature effects of this smoke are important parts of the study of nuclear winter. Second, it is useful to have some actual observations of the effects of smoke to compare to theoretical models of nuclear winter. Extensive urban and industrial smoke plumes are not readily available for study. Each year, however, a number of forest fires are generated by lightning, in some cases producing extensive smoke plumes. Anecdotal observations from extensive Siberian forest fires in 1915 (*4*) and Canadian forest fires in 1950 (*5*) indicated a daytime surface cooling of several degrees Celsius. In addition, Robock (*6*) found similar surface temperature effects of forest fire smoke plumes over the midwestern United States in the summers of 1981 and 1982 and over Alaska in May 1987 by examining objective errors of numerical temperature forecasts. In all these cases, elevated smoke layers produced daytime cooling but had no nighttime effects. I now describe a feedback process that produced much larger and longer lasting surface temperature effects, caused by smoke from forest fires in northern California in September 1987. Smoke was trapped in valleys for more than 1 week by an inversion that was strengthened by the cooling.

On 30 August 1987, orographic thunderstorms in northern California and southern Oregon ignited severe forest fires that burned for more than 1 month, consuming 203 km$^2$ of forest. (This is less than 0.1% of the area that might burn in a nuclear holocaust.) For the first 2 weeks of the fires, except for the time when a weak cold front passed over the area on 2 September, a high-pressure system prevailed over the region. The result was a subsidence inversion, which trapped smoke in the mountain valleys, particularly in Klamath River Canyon, which extends from Happy Camp at the north to Orleans at the south (Fig. 1). Each day, more smoke accumulated beneath the inversion, with the surface cooling produced by the blockage of sunlight strengthening the inversion and trapping more smoke (*7*). Because the smoke has a higher albedo than the wooded surface (Fig. 2d), the result is a net cooling of the entire atmosphere-surface system. Virtually all the sunlight that is not reflected by the smoke is absorbed before it reaches the ground, thereby strongly cooling the ground while slightly heating the air, although not enough to destabilize the air with respect to the synoptic scale inversion. This positive feedback effect of the smoke enhanced both the amplitude and the duration of the cooling.

I examined surface air temperature data for the region between 39°N and 45°N and west of 120°W to the Pacific Ocean, in northern California and southwestern Oregon (Fig. 1), using data from 96 National Weather Service stations for which 30-year normals have been computed (*8*), another 65 National Weather Service climatological observing stations (*9*), and 85 Forest Service stations (*10*), for a total of 246 stations. Not all of these stations made observations each day during this period, but for September it was possible to use more than 70 stations in the region to calculate deviations from normal and more than 200 stations to calculate

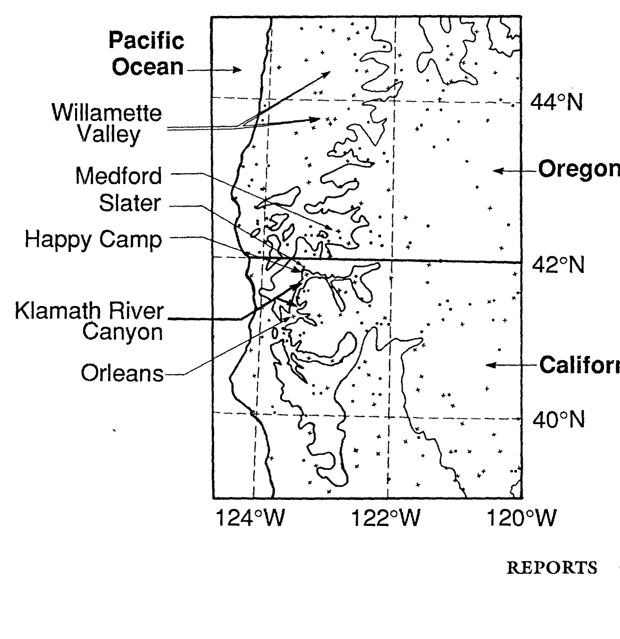


**Fig. 1.** Map of the study area in northern California and southern Oregon. Stations for which normals are available are plotted as crosses, and the remaining stations are plotted as dots. Contour of 1000-m elevation and observation stations mentioned in the text and Figs. 3 and 4 are shown.

Department of Meteorology, University of Maryland, College Park, MD 20742.